THE PUBLISHING HOUSE
OF THE ROMANIAN ACADEMY

*PROCEEDINGS OF THE ROMANIAN ACADEMY, Series A,*
*Volume 25, Number 1/2024, pp. 65–74*
DOI:

# PATH AND TRAJECTORY PLANNING OF A RPRPR PLANAR PARALLEL ROBOT FOR PREVENTION OF HIGH-ORDER SINGULARITIES

Mustafa ÖZDEMİR [1], Levent KARAKAYA [2]

[1] Marmara University, Faculty of Engineering, Department of Mechanical Engineering,
Recep Tayyip Erdoğan Campus, 34854 Maltepe, İstanbul, Türkiye
[2] Marmara University, Institute of Pure and Applied Sciences, Department of Mechanical Engineering (English),
Göztepe Campus, 34722 Kadıköy, İstanbul, Türkiye
Corresponding author: Mustafa ÖZDEMİR, E-mail: mustafa.ozdemir@marmara.edu.tr
[1] ORCID iD: https://orcid.org/0000-0002-4981-9573; [2] ORCID iD: https://orcid.org/0000-0002-3896-8194

**Abstract**. Parallel robots have many remarkable advantages over their conventional serial counterparts. Highly accurate positioning capability and high payload-to-weight ratio are among the main ones. The main factor underlying all these advantages is their closed-loop construction. However, this constructional feature also causes a special singularity problem, which constitutes their biggest disadvantage. Characteristic singularities classified as Type II exist inside their workspace, around which the magnitude of the inverse dynamic solution grows unboundedly. This naturally yields the saturation of the actuators and eventually in uncontrollability of the robot. Consequently, the whole workspace becomes impossible to be used. In order to pass through a Type II singularity, the consistency of the motion equations of the robot must be maintained at that singularity. However, any Type II singular configuration can transform into a high-order singularity, which, in order to be passed through, requires additional conditions other than the consistency. Therefore, full utilization of the whole workspace with a minimum number of conditions requires to avoid high-order singularities. The present article contributes to the literature by developing path and trajectory planning principles for preventing a two-degree-of-freedom planar parallel robot with RPRPR structure from experiencing high-order singularities.

***Key words**:* parallel robot, path planning, trajectory planning, singularity, high-order singularity.

## 1. INTRODUCTION

Thanks to their closed-loop structure, parallel mechanisms have many important capabilities such as highly accurate positioning, working under high loads, and performing high-speed and high-acceleration tasks [1, 2]. For these reasons, they are more and more preferred in simulator technologies [3, 4], industrial robots [5, 6], machining [7–9], additive manufacturing [10, 11], medical and surgical robotics [12–14].

The biggest disadvantage of parallel robots compared to their conventional serial counterparts is that there exist Type II singularities inside their workspace [15]. Around these singularities, the magnitude of the inverse dynamic solution diverges to infinity. Accordingly, the actuators get saturated, and the robot becomes uncontrollable [16]. Based on these dynamical aspects, they are also called drive singularities [17] or actuation singularities [17, 18].

As can be appreciated from the consequences mentioned above, Type II singularities cause a parallel robot to use only a small part of its workspace, and for this reason, they have been the subject of many studies in the literature. Initially, studies had generally focused on determining the loci of these singularities [19–22]. This is because it was common practice at the time to avoid singularities when planning paths [23, 24]. Over time, however, the focus has shifted more to developing methods that will enable parallel robots to pass through them. A condition to be met in this regard is that the motion equations of the robot must be consistent at the singularity to be crossed [17, 25, 26].

However, as shown by Özdemir [27], parallel robots may also encounter singularities that require additional conditions besides consistency in order to be passed through. These singularities are high-order

singularities of parallel robots [28]. Any Type II singular configuration can transform into a high-order singularity depending on the path and trajectory of the end-effector [27–29].

High-order singularities of parallel robots are much more critical than their classical Type II singularities, as they are much more difficult to remove by requiring a greater number of conditions to be met. In this sense, avoidance of high-order singularities has a key role in the optimization of the desingularization process of parallel robots. The present article contributes to the literature by establishing the path and trajectory design principles of high-order singularity prevention for a two-degree-of-freedom planar parallel robot with RPRPR structure where R and P denote revolute and prismatic joints, respectively. This closed kinematic chain belongs to the classical five-bar family and it is one of the mostly used planar parallel robot architectures with two common actuation schemes, namely R<u>P</u>R<u>P</u>R and <u>R</u>PR<u>P</u><u>R</u> [30] where the underlines show the actuated joints. The <u>R</u>PR<u>P</u><u>R</u> architecture is considered in the present study.

## 2. EQUATIONS OF MOTION

The robot under study is shown in Fig. 1. The fixed Cartesian coordinate system $xy$ has its origin at point $A$. Point $E$ is the endpoint of the robot, and $x_E$ and $y_E$ are its horizontal and vertical Cartesian coordinates, respectively. The torques provided to the robot by the motors at joints $A$ and $B$ are $T_1$ and $T_2$, respectively. Link 1 is the fixed link whereas links 2, 3, 4 and 5 are the moving links. The length of the fixed link is $a_1 = |AB|$. The prismatic joint variables are $s_1 = |AE|$ and $s_2 = |BE|$. The revolute joint variables $\theta_1$ and $\theta_2$ are defined on the figure. The gravity acceleration $g$ is taken to be along the negative $y$-axis. Link $i$ ($i = 2, 3, 4, 5$) has mass $m_i$, mass center $G_i$, and centroidal mass moment of inertia $I_i$. The distances used to express the positions of the moving mass centers are as follows: $r_2 = |AG_2|$, $r_3 = |EG_3|$, $r_4 = |BG_4|$ and $r_5 = |EG_5|$.

The velocity loop equations can be written as

$$\mathbf{J}\dot{\mathbf{q}} = \begin{bmatrix} 0 \\ 0 \end{bmatrix} \tag{1}$$

where

$$\mathbf{q} = \begin{bmatrix} \theta_1 \\ s_1 \\ \theta_2 \\ s_2 \end{bmatrix} \tag{2}$$

$$\mathbf{J} = \begin{bmatrix} -s_1 \sin(\theta_1) & \cos(\theta_1) & s_2 \sin(\theta_2) & -\cos(\theta_2) \\ s_1 \cos(\theta_1) & \sin(\theta_1) & -s_2 \cos(\theta_2) & -\sin(\theta_2) \end{bmatrix} \tag{3}$$

The equations of motion of the robot can be expressed in joint space as

$$\mathbf{M}\ddot{\mathbf{q}} + \mathbf{N} = \mathbf{Q} + \mathbf{J}^T\boldsymbol{\lambda} \tag{4}$$

where

$$\mathbf{M} = \begin{bmatrix} M_{11} & 0 & 0 & 0 \\ 0 & M_{22} & 0 & 0 \\ 0 & 0 & M_{33} & 0 \\ 0 & 0 & 0 & M_{44} \end{bmatrix} \tag{5}$$

$$\mathbf{N} = \begin{bmatrix} N_1 \\ N_2 \\ N_3 \\ N_4 \end{bmatrix} \tag{6}$$

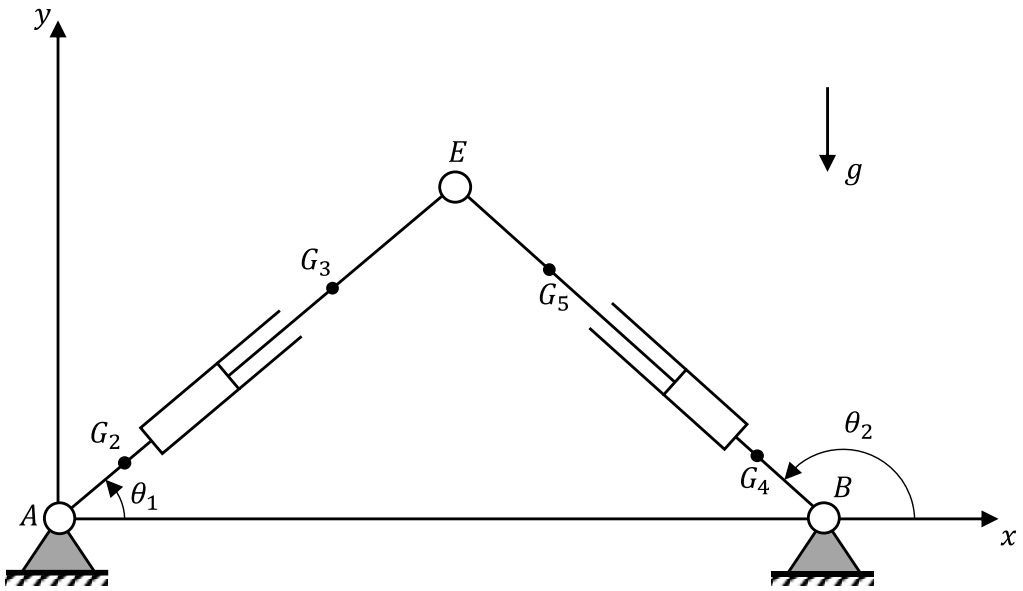


Fig. 1 – A RPRPR planar parallel robot.

The diagonal elements of **M** and the elements of **N** are given by

$$M_{11} = m_2 {r_2}^2 + I_2 + m_3(s_1 - r_3)^2 + I_3 \tag{7}$$

$$M_{22} = m_3 \tag{8}$$

$$M_{33} = m_4 {r_4}^2 + I_4 + m_5(s_2 - r_5)^2 + I_5 \tag{9}$$

$$M_{44} = m_5 \tag{10}$$

$$N_1 = 2m_3 \dot{s}_1 \dot{\theta}_1 (s_1 - r_3) + \big(m_2 r_2 + m_3(s_1 - r_3)\big) g \cos(\theta_1) \tag{11}$$

$$N_2 = -m_3(s_1 - r_3){\dot{\theta}_1}^2 + m_3 g \sin(\theta_1) \tag{12}$$

$$N_3 = 2m_5 \dot{s}_2 \dot{\theta}_2 (s_2 - r_5) + \big(m_4 r_4 + m_5(s_2 - r_5)\big) g \cos(\theta_2) \tag{13}$$

$$N_4 = -m_5(s_2 - r_5){\dot{\theta}_2}^2 + m_5 g \sin(\theta_2) \tag{14}$$

**Q** is the vector of generalized nonconservative forces. We assume that the motor torques are the only external torques and no other external nonconservative forces or moments act on the robot. Then

$$\mathbf{Q} = \begin{bmatrix} T_1 \\ 0 \\ T_2 \\ 0 \end{bmatrix} \tag{15}$$

**λ** is the vector of Lagrange multipliers of the form

$$\boldsymbol{\lambda} = \begin{bmatrix} \lambda_1 \\ \lambda_2 \end{bmatrix} \tag{16}$$

## 3. HIGH-ORDER SINGULARITIES AND ESTABLISHMENT OF PATH AND TRAJECTORY PLANNING PRINCIPLES FOR PREVENTING THEM

It is seen from equation (15) that the elements of $\mathbf{Q}$ that correspond to the unactuated joint variables are equal to zero. Based on this fact, equation (4) can be separated into two parts as follows:

$$\mathbf{M}_a\ddot{\mathbf{q}} + \mathbf{N}_a = \mathbf{Q}_a + (\mathbf{J}_a)^T\boldsymbol{\lambda} \tag{17}$$

$$\mathbf{M}_u\ddot{\mathbf{q}} + \mathbf{N}_u = \mathbf{Q}_u + (\mathbf{J}_u)^T\boldsymbol{\lambda} \tag{18}$$

where

$$\mathbf{M}_a = \begin{bmatrix} M_{11} & 0 & 0 & 0 \\ 0 & 0 & M_{33} & 0 \end{bmatrix} \tag{19}$$

$$\mathbf{M}_u = \begin{bmatrix} 0 & M_{22} & 0 & 0 \\ 0 & 0 & 0 & M_{44} \end{bmatrix} \tag{20}$$

$$\mathbf{N}_a = \begin{bmatrix} N_1 \\ N_3 \end{bmatrix} \tag{21}$$

$$\mathbf{N}_u = \begin{bmatrix} N_2 \\ N_4 \end{bmatrix} \tag{22}$$

$$\mathbf{J}_a = \begin{bmatrix} -s_1\sin(\theta_1) & s_2\sin(\theta_2) \\ s_1\cos(\theta_1) & -s_2\cos(\theta_2) \end{bmatrix} \tag{23}$$

$$\mathbf{J}_u = \begin{bmatrix} \cos(\theta_1) & -\cos(\theta_2) \\ \sin(\theta_1) & -\sin(\theta_2) \end{bmatrix} \tag{24}$$

$$\mathbf{Q}_a = \begin{bmatrix} T_1 \\ T_2 \end{bmatrix} \tag{25}$$

$$\mathbf{Q}_u = \begin{bmatrix} 0 \\ 0 \end{bmatrix} \tag{26}$$

Hence, provided that the matrix $(\mathbf{J}_u)^T$ is invertible, equation (18) can be solved for $\boldsymbol{\lambda}$ as

$$\boldsymbol{\lambda} = [(\mathbf{J}_u)^T]^{-1}(\mathbf{M}_u\ddot{\mathbf{q}} + \mathbf{N}_u) \tag{27}$$

Then, the required motor torques can be computed as

$$\begin{bmatrix} T_1 \\ T_2 \end{bmatrix} = \mathbf{M}_a\ddot{\mathbf{q}} + \mathbf{N}_a - (\mathbf{J}_a)^T[(\mathbf{J}_u)^T]^{-1}(\mathbf{M}_u\ddot{\mathbf{q}} + \mathbf{N}_u) \tag{28}$$

When the determinant of $(\mathbf{J}_u)^T$ vanishes at a point, a Type II singularity occurs at that point [17]. Thus, Type II singularities of the robot can be determined from

$$\delta = \det((\mathbf{J}_u)^T) = \sin(\theta_1 - \theta_2) = 0 \tag{29}$$

It can be seen by inspecting the geometry of the robot that there are three possible cases at a Type II singularity. These are presented in Table 1. Notice that $(\mathbf{J}_u)^T$ becomes rank-deficient by one at Type II singularities of the robot.

*Table 1*

Three different cases of Type II singular configurations of the robot:

| Type II singularity case | Values of the joint variables |
|---|---|
| 1 | $\theta_1 = \theta_2 = 0$ |
| 2 | $\theta_1 = \theta_2 = \pi$ |
| 3 | $\theta_1 = 0$ and $\theta_2 = \pi$ |

Equation (27) gives

$$\lambda_1 = \frac{\mu_1}{\delta} \tag{30}$$

$$\lambda_2 = \frac{\mu_2}{\delta} \tag{31}$$

where

$$\mu_1 = -\sin(\theta_2)\,(M_{22}\ddot{s}_1 + N_2) - \sin(\theta_1)\,(M_{44}\ddot{s}_2 + N_4) \tag{32}$$

$$\mu_2 = \cos(\theta_2)\,(M_{22}\ddot{s}_1 + N_2) + \cos(\theta_1)\,(M_{44}\ddot{s}_2 + N_4) \tag{33}$$

The condition that the robot must satisfy for maintaining consistency of its equations of motion at a singularity can be determined as follows:

$$\sigma(M_{22}\ddot{s}_1 + N_2) + M_{44}\ddot{s}_2 + N_4 = 0 \tag{34}$$

where the values of σ are provided in Table 2.

*Table 2*

Values of σ

| Type II singularity case | σ |
|---|---|
| 1 | 1 |
| 2 | 1 |
| 3 | −1 |

Satisfaction of equation (34) at the singularity time $t_s$ is equivalent to satisfaction of

$$\mu_1(t_s) = \mu_2(t_s) = 0 \tag{35}$$

So, if the trajectory is consistent, then

$$\lambda_1(t_s) = \lambda_2(t_s) = \frac{0}{0} \tag{36}$$

Note that $\mu_1(t_s) = 0$ is automatically satisfied for the robot under study. But to have $\mu_2(t_s) = 0$, equation (34) must be satisfied at the singularity.

The boundedness of the inverse dynamic solution requires the limits $\lim_{t\to t_s}\lambda_1$ and $\lim_{t\to t_s}\lambda_2$ to be finite. Equation (36) suggests the application of l'Hôpital's Rule as:

$$\lim_{t\to t_s}\lambda_1 = \lim_{t\to t_s}\frac{\frac{\mathrm{d}\mu_1}{\mathrm{d}t}}{\frac{\mathrm{d}\delta}{\mathrm{d}t}} \tag{37}$$

$$\lim_{t\to t_s}\lambda_2 = \lim_{t\to t_s}\frac{\frac{\mathrm{d}\mu_2}{\mathrm{d}t}}{\frac{\mathrm{d}\delta}{\mathrm{d}t}} \tag{38}$$

Equations (37) and (38) show that if $\mathrm{d}\delta/\mathrm{d}t$ vanishes at time $t = t_s$, then extra conditions other than consistency must be satisfied for a bounded inverse dynamic solution. This means that in order the robot to have a high-order singularity, it is required that

$$\left.\frac{\mathrm{d}\delta}{\mathrm{d}t}\right|_{t=t_s} = 0 \tag{39}$$

Recalling that sine and cosine of an angle cannot be simultaneously equal to zero, this high-order singularity condition can be equivalently expressed as

$$\dot{\theta}_1(t_s) - \dot{\theta}_2(t_s) = 0 \tag{40}$$

The velocity inverse kinematics solution gives

$$\dot{\theta}_1 = -\frac{\sin(\theta_1)}{s_1}\dot{x}_E + \frac{\cos(\theta_1)}{s_1}\dot{y}_E \tag{41}$$

$$\dot{\theta}_2 = -\frac{\sin(\theta_2)}{s_2}\dot{x}_E + \frac{\cos(\theta_2)}{s_2}\dot{y}_E \tag{42}$$

In this study, we assume that there are no inverse kinematic singularities; hence $s_1$ and $s_2$ are always nonzero throughout the motion.

$$\dot{\theta}_1(t_s) = \frac{\psi}{s_1(t_s)}\dot{y}_E(t_s) \tag{43}$$

$$\dot{\theta}_2(t_s) = \sigma\frac{\psi}{s_2(t_s)}\dot{y}_E(t_s) \tag{44}$$

where the values of ψ are provided in Table 3.

*Table 3*

Values of ψ

| Type II singularity case | ψ |
|---|---|
| 1 | 1 |
| 2 | −1 |
| 3 | 1 |

Substituting equations (43) and (44) into equation (40), we get

$$\psi\left(\frac{1}{s_1(t_s)} - \sigma\frac{1}{s_2(t_s)}\right)\dot{y}_E(t_s) = 0 \tag{45}$$

or

$$-\sigma\frac{a_1\dot{y}_E(t_s)}{s_1(t_s)s_2(t_s)} = 0 \tag{46}$$

Equation (46) reveals that a high-order singularity of the robot under investigation occurs when

$$\dot{y}_E(t_s) = 0 \tag{47}$$

The condition given by equation (47) implies that a Type II singular configuration becomes of high order if the trajectory is such that the endpoint $E$ has zero velocity at the singularity time or if the endpoint path is such that it has a horizontal tangent at that singular configuration; that is, if the following equation holds:

$$\left.\frac{dy_E}{dx_E}\right|_{t=t_s} = 0 \tag{48}$$

Hence, the path design principle to avoid the occurrence of a high-order singularity of the RPRPR robot is that the endpoint path must have a nonzero slope at the Type II singular configurations. Additionally, the trajectory design principle in this regard is that the endpoint must have a nonzero velocity at Type II singularities. These path and trajectory design principles are quite easy to implement in practice.

## 4. NUMERICAL EXAMPLES

To illustrate the application of our findings, let us consider an RPRPR robot with $a_1 = 6$ m. The task is to move the endpoint $E$ along a cubic path from $(x, y) = (2\text{ m}, -1\text{ m})$ to $(x, y) = (4\text{ m}, 1\text{ m})$ in $t_f = 5$ s. It is worth noting that the robot will inevitably pass through a Type II singular configuration because the endpoint path will cross the $x$-axis during the realization of this task. At the initial configuration, the joint variables are as follows: $\theta_1 = -26.5651°$, $s_1 = 2.2361$ m, $\theta_2 = -165.9638°$ and $s_2 = 4.1231$ m. The starting and ending velocities and accelerations are zero. In accordance with the task requirements, the $x$-coordinate trajectory of the endpoint is generated by the following quintic polynomial of time $t$:

$$x_E(t) = 2 + \frac{4}{25}t^3 - \frac{6}{125}t^4 + \frac{12}{3125}t^5 \tag{49}$$

This equation is plotted in Fig. 2. From equation (49) it can be deduced that $\dot{x}_E > 0$ for all $t$ in the open interval from 0 to 5 s. This guarantees that the endpoint will have a nonzero velocity when the Type II singularity occurs.

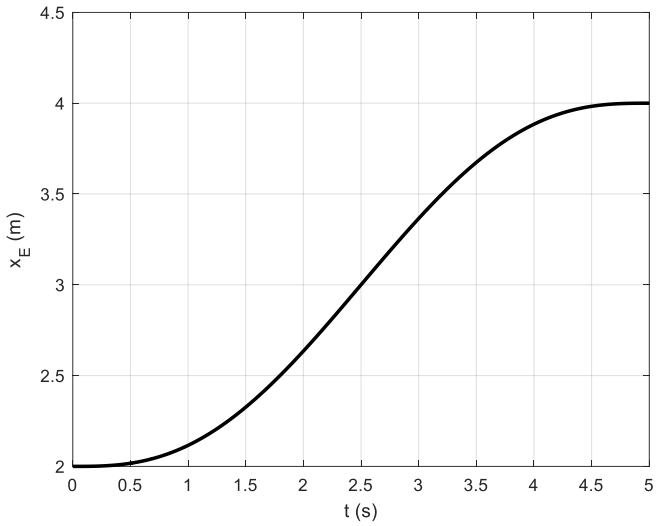


Fig. 2 – The $x$-coordinate trajectory of the endpoint.

As a first example, let us take the endpoint path given by

$$y = x^3 - 9x^2 + 27x - 27 \tag{50}$$

This path is the path 1 in Fig. 3, and it connects the required starting and ending positions of the endpoint. There are no inverse kinematic singularities along this path, but a Type II singular configuration occurs when the endpoint arrives at the point $(x, y) = (3\text{ m}, 0)$ at time $t = 2.5$ s. So, $t_s = 2.5$ s.

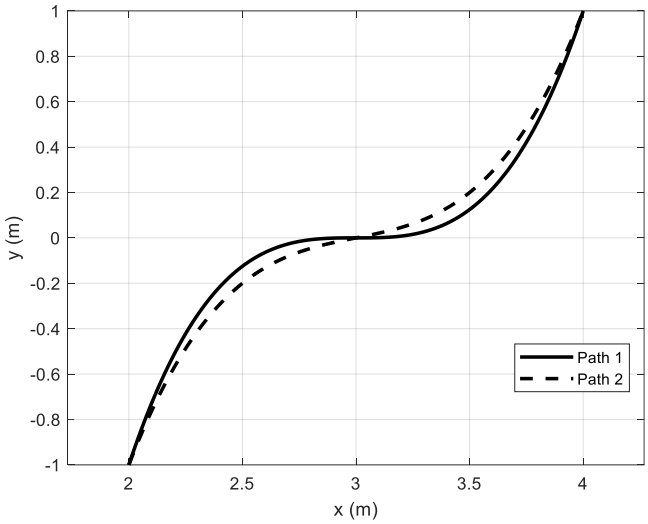


Fig. 3 – Endpoint paths considered in the examples.

The singularity encountered in this first example is of high order since we have $\delta(t_s) = \dot{\delta}(t_s) = \ddot{\delta}(t_s) = 0$ (see Fig. 4). This is because path 1 has zero slope and curvature at the singular point $(x, y) = (3\text{ m}, 0)$.

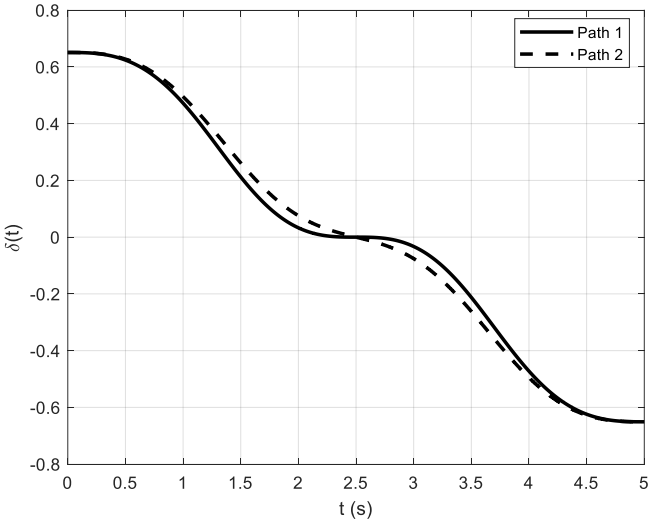


Fig. 4 – Variations of the determinant δ over time in the examples with path 1 and path 2.

To prevent the singularity from transforming into a high-order singularity, the path planning principle introduced in this article must be applied. To show this, in our second example the endpoint path is slightly modified to have a nonzero slope at the singular point, namely, to have a slope of 0.2 at the point $(x, y) = (3\text{ m}, 0)$. The new path is the path 2 in Fig. 3 and is given by

$$y = 0.8x^3 - 7.2x^2 + 21.8x - 22.2 \tag{51}$$

In this second example with path 2 there are again no inverse kinematic singularities, and the same Type II singular configuration is encountered again at the same time $t = 2.5$ s. However, this singular configuration is now not a high-order singularity since the first-order time derivative of the determinant δ at the singularity time is not equal to zero (see Fig. 4). Figure 5 shows the actuated joint variables required to follow path 2 in the second example.

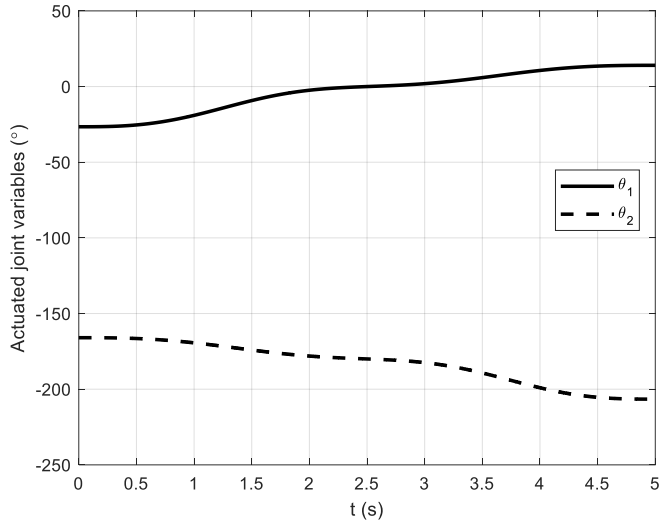


Fig. 5 – Variation of the actuated joint variables over time in the second example with path 2.

## 5. CONCLUSIONS

The present article contributes to the literature by deriving the high-order singularity condition of a five-link planar parallel robot with RPRPR architecture. It is shown that any Type II singular configuration of this robot transforms into a high-order singularity if the slope of the endpoint path is zero at that singular configuration or if the endpoint velocity is zero at the singularity time. The occurrence of a high-order singularity can be prevented by properly planning the endpoint path and trajectory in accordance with these findings.

The application and effectiveness of these path and trajectory design principles are illustrated by numerical examples. These examples demonstrate that transformation of a Type II singularity of the RPRPR planar parallel robot into a high-order singularity can be avoided by planning the endpoint path to have a nonzero slope at the singular point and, additionally, by ensuring that the endpoint has a nonzero velocity at the singularity time. In order to better understand the practical importance of the results of this article, it should be recalled that it is necessary to pass through Type II singular configurations for fully utilizing the whole workspace of RPRPR planar parallel robots, and this can be achieved without any additional conditions other than consistency if and only if the occurrence of high-order singularities is prevented.

## ACKNOWLEDGEMENTS

This article is based on a part of the Master of Science Thesis of the second author (Levent KARAKAYA) in the Department of Mechanical Engineering (English) at Marmara University Institute of Pure and Applied Sciences under the supervision of the first author (Assoc. Prof. Dr. Mustafa ÖZDEMİR).

## REFERENCES

1. J.-P. MERLET, *Parallel Robots*, Second Edition, in: G.M.L. GLADWELL (Ed.), Solid Mechanics and Its Applications, vol. 128, Springer, 2006.
2. Y. JIN, H. CHANAL, F. PACCOT, Parallel Robots, in: A.Y.C. NEE (Ed.), *Handbook of Manufacturing Engineering and Technology*, Springer-Verlag London, 2015, pp. 2091–2127.
3. B. REN, Z. ZHANG, *Design of 4PUS-PPPS redundant parallel mechanism oriented to the visual system of flight simulator*, International Journal of Intelligent Robotics and Applications, **5**, *4*, pp. 534–542, 2021.

4. C. NGUYEN MANH, N.T. NGUYEN, N. BUI DUY, T.L. NGUYEN, *Adaptive fuzzy Lyapunov-based model predictive control for parallel platform driving simulators*, Transactions of the Institute of Measurement and Control, **45**, *5*, pp. 838–852, 2023.
5. J.S. TOQUICA, P.S. OLIVEIRA, W.S.R. SOUZA, J.M.S.T. MOTTA, D.L. BORGES, *An analytical and a Deep Learning model for solving the inverse kinematic problem of an industrial parallel robot*, Computers & Industrial Engineering, **151**, p. 106682, 2021.
6. H.-C. HUANG, Y.-X. CHEN, *Evolutionary optimization of fuzzy reinforcement learning and its application to time-varying tracking control of industrial parallel robotic manipulators*, IEEE Transactions on Industrial Informatics, **19**, *12*, pp. 11712–11720, 2023.
7. Z. XIE, F. XIE, X.-J. LIU, J. WANG, B. MEI, *Tracking error prediction informed motion control of a parallel machine tool for high-performance machining*, International Journal of Machine Tools and Manufacture, **164**, p. 103714, 2021.
8. P. YAN, H. HUANG, B. LI, D. ZHOU, *A 5-DOF redundantly actuated parallel mechanism for large tilting five-face machining*, Mechanism and Machine Theory, **172**, p. 104785, 2022.
9. M. WANG, Y. SONG, B. LIAN, P. WANG, K. CHEN, T. SUN, *Dimensional parameters and structural topology integrated design method of a planar 5R parallel machining robot*, Mechanism and Machine Theory, **175**, p. 104964, 2022.
10. J. HUANG, B. ZHANG, J. XIAO, Q. ZHANG, *An approach to improve the resolution of DLP 3D printing by parallel mechanism*, Applied Sciences, **12**, *24*, p. 12905, 2022.
11. T.S. TAMIR, G. XIONG, X. DONG, Q. FANG, S. LIU, E. LODHI, Z. SHEN, F.-Y. WANG, *Design and optimization of a control framework for robot assisted additive manufacturing based on the Stewart platform*, International Journal of Control, Automation and Systems, **20**, *3*, pp. 968–982, 2022.
12. B. GHERMAN, I. BIRLESCU, N. PLITEA, G. CARBONE, D. TARNITA, D. PISLA, *On the singularity-free workspace of a parallel robot for lower-limb rehabilitation*, Proceedings of the Romanian Academy, Series A: Mathematics, Physics, Technical Sciences, Information Science, **20**, *4*, pp. 383–391, 2019.
13. D. PISLA, D. TARNITA, P. TUCAN, N. TOHANEAN, C. VAIDA, I.D. GEONEA, G. BOGDAN, C. ABRUDAN, G. CARBONE, N. PLITEA, *A parallel robot with torque monitoring for brachial monoparesis rehabilitation tasks*, Applied Sciences, **11**, *21*, p. 9932, 2021.
14. D. PISLA, I. BIRLESCU, A. PUSCA, P. TUCAN, B. GHERMAN, A. PISLA, T. ANTAL, C. VAIDA, *Kinematics and workspace analysis of an innovative 6-DOF parallel robot for SILS*, Proceedings of the Romanian Academy, Series A: Mathematics, Physics, Technical Sciences, Information Science, **23**, *3*, pp. 277–286, 2022.
15. C. GOSSELIN, J. ANGELES, *Singularity analysis of closed-loop kinematic chains*, IEEE Transactions on Robotics and Automation, **6**, *3*, pp. 281–290, 1990.
16. P. CHOUDHURY, A. GHOSAL, *Singularity and controllability analysis of parallel manipulators and closed-loop mechanisms*, Mechanism and Machine Theory, **35**, *10*, pp. 1455–1479, 2000.
17. S.K. IDER, *Inverse dynamics of parallel manipulators in the presence of drive singularities*, Mechanism and Machine Theory, **40**, *1*, pp. 33–44, 2005.
18. M.K. OZGOREN, *Kinematic and kinetostatic analysis of parallel manipulators with emphasis on position, motion, and actuation singularities*, Robotica, **37**, *4*, pp. 599–625, 2019.
19. J.-P. MERLET, *Singular configurations of parallel manipulators and Grassmann geometry*, The International Journal of Robotics Research, **8**, *5*, pp. 45–56, 1989.
20. B.M. ST-ONGE, C.M. GOSSELIN, *Singularity analysis and representation of the general Gough-Stewart platform*, The International Journal of Robotics Research, **19**, *3*, pp. 271–288, 2000.
21. R. DI GREGORIO, *Singularity-locus expression of a class of parallel mechanisms*, Robotica, **20**, *3*, pp. 323–328, 2002.
22. I.A. BONEV, D. ZLATANOV, C.M. GOSSELIN, *Singularity analysis of 3-DOF planar parallel mechanisms via screw theory*, ASME Journal of Mechanical Design, **125**, *3*, pp. 573–581, 2003.
23. S. BHATTACHARYA, H. HATWAL, A. GHOSH, *Comparison of an exact and an approximate method of singularity avoidance in platform type parallel manipulators*, Mechanism and Machine Theory, **33**, *7*, pp. 965–974, 1998.
24. S. SEN, B. DASGUPTA, A.K. MALLIK, *Variational approach for singularity-free path-planning of parallel manipulators*, Mechanism and Machine Theory, **38**, *11*, pp. 1165–1183, 2003.
25. C.K.K. JUI, Q. SUN, *Path tracking of parallel manipulators in the presence of force singularity*, ASME Journal of Dynamic Systems, Measurement, and Control, **127**, *4*, pp. 550–563, 2005.
26. S. BRIOT, V. ARAKELIAN, *Optimal force generation in parallel manipulators for passing through the singular positions*, The International Journal of Robotics Research, **27**, *8*, pp. 967–983, 2008.
27. M. ÖZDEMİR, *Removal of singularities in the inverse dynamics of parallel robots*, Mechanism and Machine Theory, **107**, pp. 71–86, 2017.
28. M. ÖZDEMİR, *High-order singularities of 5R planar parallel robots*, Robotica, **37**, *2*, pp. 233–245, 2019.
29. M. ÖZDEMİR, *Hypersingularities of 3-RRR planar parallel robots*, Proceedings of the Romanian Academy, Series A: Mathematics, Physics, Technical Sciences, Information Science, **22**, *4*, pp. 353–360, 2021.
30. H.F. QUINTERO, L.A. MEJIA, M. DIAZ-RODRIGUEZ, *End-effector positioning due to joint clearances: A comparison among three planar 2-DOF parallel manipulators*, Journal of Mechanical Science and Technology, **33**, *7*, pp. 3497–3507, 2019.

*Received April 10, 2023*